

Published in final edited form as:

Appl Opt. 2009 January 10; 48(2): 221–228.

Fundus camera systems: a comparative analysis

Edward DeHoog^{1,*} and James Schwiegerling^{1,2,3}

¹Biomedical Engineering Program, University of Arizona, 1657 E. Helen St., Tucson, Arizona 85721, USA

²Ophthalmology and Vision Sciences, University of Arizona, 655 N. Alvernon Way, Suite 108 Tucson, Arizona 85711, USA

³College of Optical Science, University of Arizona, 1630 E. University Boulevard, Tucson, Arizona 85721, USA

Abstract

Retinal photography requires the use of a complex optical system, called a fundus camera, capable of illuminating and imaging the retina simultaneously. The patent literature shows two design forms but does not provide the specifics necessary for a thorough analysis of the designs to be performed. We have constructed our own designs based on the patent literature in optical design software and compared them for illumination efficiency, image quality, ability to accommodate for patient refractive error, and manufacturing tolerances, a comparison lacking in the existing literature.

1. Background

A fundus camera is a complex optical system used for imaging the retina of the eye. Retinal imaging presents a unique difficulty considering that the retina must be illuminated and imaged simultaneously, a process which forces illumination and imaging systems to share a common optical path [1-3]. Because the retina is a minimally reflective surface, the power of the back reflections from the shared optics of the illumination and imaging paths is greater than the power reflected by the retina [4-6]. Examination of the patent literature shows two dominate design forms used to overcome these challenges [1,2]. What is missing from the literature is an evaluation of which system performs better at retinal imaging in terms of optical imaging and illumination performance criteria. While patent literature shows these design forms, these patents lack specification for the optical layout, such as lens powers, spacings, and conjugate planes. Consequently, performing illumination and imaging analysis on these designs are impossible. We have designed systems based on the schematics in the patent literature and carried out a thorough analysis to better understand the engineering aspects of fundus cameras.

The authors' designs in Figs. 1(a) and 1(b) are adapted for the schematics in the patent literature. Analysis of these systems shows the general principles involved in designing fundus cameras. A source (elements 11a and 12b) is imaged onto the pupil of the eye allowing the retina to be illuminated. Corneal back reflections are eliminated by placing a central obscuration in the illumination system conjugate to the pupil of the eye (elements 9a and 10b). Placement of this component results in an annular illumination pattern at the pupil of the eye. The imaging system consists of an objective lens and a simple zoom lens (elements 3a, 5a, 6a, 2b, 4b, and 5b). The objective lens forms an intermediate image of the retina in front of the zoom lens, which

reimages the retina onto the camera (elements 7a and 6b) while accommodating for the patient's refractive error [1-3].

The two cameras presented in Fig. 1 differ only in their implementation of the design principles. The fundus camera with the external illumination design in Fig. 1(a) uses a beam splitter (element 2a) placed in front of the eye (element 1a) to combine the illumination and imaging systems. A source is imaged onto the pupil of the eye by lenses 8a and 10a. An annulus, 9a, is placed between the lenses and positioned conjugate to the pupil of the eye [2]. The second design form in Fig. 1(b), an internal illumination design, uses a mirror with a central hole, element 3b, placed conjugate to the pupil of eye to combine the illumination and imaging systems. The illumination and imaging path sharing the objective, element 2b, requires a more complicated system to eliminate back reflections. The source, 12b, is reimaged to the mirror by lenses 7b, 9b, and 11b. Back reflections from the front and back surfaces of the objective are removed by a black dot, element 8b, and placed conjugate to the back surface of the objective [1,3]. The internal system uses a single aspheric objective to reduce the number of surfaces contributing to the back reflections, whereas the objective in the external system can consist of multiple elements because it is not part of the illumination pathway and will not contribute to back reflections. The only difference in the imaging path of both systems is the existence of a baffle, 4a. This baffle, placed conjugate to the pupil of the eye, helps reduce corneal back reflections and limits the entrance pupil diameter of the imaging system. In the internal system, the mirror with the central hole serves the same purpose as the baffle in the external system. An iris can be placed immediately behind the mirror with the central hole to allow for further control of the entrance pupil diameter and for elimination of back reflections. Both systems provide different solutions to the unique problem of imaging the retina.

Despite the fundus camera's existence for more than 50 years, little has changed in its design, and there is minimal information outside the patent literature about the design criteria used to evaluate its performance. Our goals are to recreate and model the two primary designs, external and internal illumination, found in the patent literature and to evaluate these models for image quality, defocus accommodation, illumination efficiency, and manufacturability.

2. Methods

A. System Specifications

The two fundus cameras discussed in the Section 1 are modeled and tested using sequential and nonsequential ray tracing in Zemax. Camera systems that are designed to have the same design specifications. Imaging systems are designed to meet the following criteria: field of view 30° , $F/\#$ 5.7, and image plane size of a 1/2 CCD camera 4.8×6.4 mm. Each imaging system is required to be able to accommodate across 95% of the population of refractive error, $-8D$ to $5D$ [7,8]. Design wavelengths 500, 587.5, and 656.3 nm are selected and weighted by the spectral reflectance of the retina resulting in the 656.3 nm wavelength being weighted six times higher than the 500 nm [4-6]. To limit the aberrations of the eye and maximize irradiance on the CCD, the entrance pupil diameter of the eye is limited to 2 mm [6,9]. Imaging systems are designed to have a polychromatic MTF value of 0.4 at 50 lp/mm, allowing for the resolution of the majority of retinal structures. Resolution of retina structures smaller than $20 \mu\text{m}$ is severely limited by the higher order aberrations present in the typical human eye [8,10,11]. Illumination systems are designed to have an object space NA of 0.45 and an image space NA of 0.3 using a 3 mm arc lamp as source. The annulus is designed to block the central 2.5 mm of the eye to reduce corneal back reflections caused by the illumination optics. The only aspheric element in both imaging systems is the objective lens in the internal system; however, both illumination systems utilize aspheric condenser lenses. To ensure manufacturability, aspheric lens are limited to one aspheric surface described by a conic constant, and guidelines presented by aspheric optic manufacturers are followed [12,13].

B. Imaging System Design and Testing

Objective design in both systems is characterized by two goals. The first goal is to form an intermediate image of the retina for the zoom system. The second is to relay the image of the pupil of the eye to a baffle to restrict the entrance pupil diameter of the imaging system and to block corneal back reflections. To accomplish this second goal, the pupil aberrations of the objective lens must be controlled to ensure that all rays pass through the intermediate image of the stop (located at the baffle, 4a, or at the mirror with central hole, 3b) with minimal vignetting [14]. The design of the zoom lens used in the fundus cameras is rather simplistic. A two lens system is sufficient for the range of accommodation and image quality.

As a preliminary test, objective diameter is determined for both systems as a function of field of view (FOV) for a fixed working distance. Minimum objective diameter is determined by paraxial calculations. The external objective is placed immediately after a thin beam splitter. Completed imaging systems are compared for complexity, image quality, and ability to accommodate for patient refractive error. Patient refractive error is modeled by placing a paraxial optic immediately in front of the eye model. The power of the paraxial optic is adjusted to match the levels of defocus found in the general population [7,8]. Movement of the zoom lens is used to compensate for the defocus of the subject, and MTF values at 50 lp/mm are recorded.

C. Illumination System Design and Efficiency Testing

The degree of difficulty involved in the illumination system varies greatly depending on the type of fundus camera. Design of the external illumination system is straight forward. One lens images the source onto the annulus, and the second lens images the annulus and source on the pupil of the eye. Design of the internal illumination system is more complicated. First, the image space NA of the lens system responsible for relaying the source to the mirror (elements 7–12) is determined. Next a system is designed to meet the required NA and places the intermediate image of the black dot on the objective. Ghost analysis is performed to ensure that the black dot prevents back reflections from the objective. The surfaces of the objective are treated as mirrors, and reflections from the objective surfaces are traced back through the illumination system. A black dot is placed at the focus of these back reflections. Back reflected light passing through the hole in the mirror is eliminated by adjusting the size of the black dot. Further ghost and stray light analysis of both fundus cameras is performed using nonsequential ray tracing. A model of the camera systems is constructed without an eye model. Lenses are given anti reflection coatings and placed in lens barrels. The beam splitter of the external system is set to 50% transmission and 50% reflection to maximize the irradiance of the retinal image on the CCD. (Calculation is based on maximizing the following equation for flux on the CCD from retina. $\Phi_{\text{CCD}} = R_{\text{BS}} T_{\text{BS}} R_{\text{retina}} \Phi_{\text{in}}$ where Φ_{CCD} is flux on the CCD, R_{BS} is the reflectance of the beam splitter, R_{retina} is the reflectance of the retina, and Φ_{in} is the initial flux.) A detector is placed at the CCD location. Rays are traced to determine if any back reflections or stray light is detected at the CCD. By adjusting the size and location of the back dot, the ghost reflections of the internal system are eliminated. Back reflections from the objective in the external system are not present. An eye model is added to the camera system. A detector with absorbing properties is placed at the retina. Rays are traced to determine whether the baffles and annuli are blocking ghost reflections and stray light from the eye model. Dimensions and locations of the baffles and annuli are adjusted accordingly. During each iteration of ray tracing and adjusting parameters, the detector at the retina is monitored to ensure full illumination of the fundus camera's FOV.

Once ghost reflections and stray light in each camera have been suppressed, the efficiency of the each fundus camera is determined. Reflective and scattering properties of the retina that are consistent with the literature are incorporated into the eye model [4-6,15]. The pupil size

of the eye is set to 7.5 mm to simulate dilation. Rays are traced to determine the efficiency of each system for the two sources used to simulate an arc lamp, a Lambertian disc and helical filament. We define efficiency as

$$\eta = \frac{\Phi_{\text{det}}}{\Phi_{\text{in}}} * 100\%, \quad (1)$$

where η is percent efficiency, Φ_{in} is the radiant flux entering the system, and Φ_{det} is the radiant flux at the detector of interest. Efficiency is computed for the illumination system (flux transfer from the source to retina), the imaging system (flux transfer from the retina to the CCD), and the entire system (flux transfer from the source to the CCD).

D. Tolerance Analysis

Tolerance analysis of the imaging systems is performed to determine the average performance of a manufactured system. Sensitivity analysis of tolerances is performed using the average geometric MTF at 50 lp/mm as the nominal criteria. A Monte Carlo simulation consisting of 100 trials is performed for each imaging system. To loosen tolerances, we have defined two sets of compensators likely to be used in a fundus camera [16,17]. The first set of compensators includes the movement of the zoom lens 5a and 4b and the back focus. The second set includes tip and tilt compensators to simulate the objectives and two lens components of the zoom lens being mounted in kinematic mounts in addition to the compensators in the first set. Tolerance values are limited to values given by several optical component manufacturers [12,13,18,19]. System tolerances are selected such that 90% of the Monte Carlo trials will perform better than 0.3 average geometric MTF at 50 cycles allowing for retinal image quality typical of the eye [8,10,11].

3. Results

A. Imaging System Design and Image Quality

The design of the imaging system for each fundus camera presents a unique set of challenges.

Given the same FOV and working distance, the use of the beam splitter results in the diameter of the external system objective being larger than the diameter of the internal system objective, as shown in Fig. 2. Enlarging the FOV requires increasing the beam splitter size, which forces the objective to be placed further away from the eye. This increase in the working distance results in increased ray height at the objective of the external system, making aberrations hard to control [14,17]. Fortunately, more lenses can be used in the external system objective to reduce aberrations without increasing back reflections, since the objective is not part of the illumination pathway. The internal system objective can be used at a reduced working distance, making aberrations easier to control. This also allows for a larger FOV at a smaller objective diameter.

Our fundus camera models are successful in meeting the design requirements. It should be noted that the external system objective requires an additional singlet to allow for control of pupil aberrations. Zoom optics for both fundus cameras are two lens systems. The internal system requires one additional element in the final lens to meet the image quality requirement.

Each completed imaging system is able to meet the image quality requirements of 0.4 MTF 50 lp/mm. Examination of the polychromatic MTF and field curvature plots in Figs. 3 and 4 shows the external system is slightly more successful at maintaining polychromatic image quality. This is due to the increased number of elements used for the aberration correction. Correction of chromatic aberration in the internal system is more difficult due to the use of a single

objective lens. The zoom lens of the internal system is left to correct chromatic aberration of the eye and the objective outside of the aperture stop, making the system harder to achromatize. An important aspect of retinal imaging in regard to image quality is whether polychromatic evaluation is misleading. The retina is more than six times more reflective in the red wavelengths than the green [5,6]. A better measure of image quality is the MTF corresponding to 656.3 nm, the wavelength that contributes the most to the image quality. Comparison of the MTF at 656.3 nm shows excellent image quality in both systems, and this meets the specification of at least 0.55 MTF at 50 lp/mm.

B. Defocus Accommodation

More than 35% of the population has refractive error, necessitating vision correction [7,8]. Patient refractive error, defocus being the most prevalent, will cause degradation in the image quality of the fundus camera [8,11]. A successful fundus camera is able to accommodate across the clinical range of defocus with minimal loss of image quality.

The ability of the fundus camera to accommodate for defocus is tested by adding defocus to the eye and adjusting the positions of the zoom lens to optimize image quality. The effect of accommodation on the MTF as a function of patient refractive error is shown in Figs. 5 and 6. Results show that both imaging systems are capable of maintaining good image quality across the clinical range of defocus with variation of around 0.2 in MTF. It is interesting to compare the travel of the zoom lenses as they accommodate for defocus, Table 1. Examination of the travel distances shows the front element of the external system requires more travel. However, the travel of the back element of this system is smaller than the travel of the back element of the internal system. Both imaging systems show a large degree of success in accommodating for a patient refractive error and maintaining image quality.

C. Fundus Camera Efficiency

Retinal imaging is complicated due to a number of factors: the location of the retina forces imaging illumination to share a common path through the pupil of the eye, the retina is minimally reflective, aberrations in the eye blur the image of the retina, the pupil of the eye restricts the amount of light that can illuminate the retina, and back reflections from the cornea and any other optical surface is likely to be significantly greater than the light reflected from the retina. The basic design principle of fundus cameras is to provide maximum illumination to the retina while eliminating back reflections [1-3,9].

Internal and external systems use different strategies for designing fundus cameras. Our simulations show the effectiveness of these different strategies and demonstrate the trade-offs involved. Efficiency measurements for each system, Table 2, show the internal system to be roughly twice as efficient at illuminating the retina as the external system. Further analysis of the systems shows the internal system design to be more efficient at illuminating and imaging the retina. This is due to the use of the beam splitter to couple the imaging and illumination system, which gives the fundus camera the ability to eliminate back reflections from the objective but results in significantly lower efficiency. Analysis of the illumination images in Figs. 7 and 8 shows a distinct variation in the illumination pattern. Use of the black dot in the internal system to eliminate objective lens back reflections results in a 17% drop in the irradiance in the center of the illumination pattern. This drop in central irradiance is not present in the external system. The ability to eliminate back reflection in the system is balanced by illumination efficiency and the distribution of irradiance.

D. Imaging System Tolerancing

Tolerance analysis must always be considered when determining which system is able to perform a specific task better. Systems with high performance metrics but extremely tight or

impossible tolerances are likely to be passed over for production or redesigned to make manufacturing easier [16,17]. As seen in Table 3, a set of tolerances for our systems is selected to meet our criteria of a least 0.3 average geometric MTF at 50 lp/mm. According to optical component manufacturers, these tolerance values are fairly standard, making production easier [12,13,18,19]. The Monte Carlo analysis in Table 4 gives insight into how the system would perform if manufactured. Given systems with defocus compensation only, more than 90% of the external systems show a performance drop of less than 11.3% whereas the internal systems show a drop of less than 25.5%. If we examine the second set of compensators in which kinematic mounts are assumed to be used for tip tilt compensation to the lenses, we see greater than 90% of the internal system will suffer a drop of less than 4.4%, whereas the external system will suffer drop of less than 6.4%. These results show that, despite having a larger number of optics, the external system is less sensitive to manufacturing tolerances. This finding is further supported by the standard deviations of the Monte Carlo trials. Results also demonstrate the ability of kinematic mounts to improve performance given a looser set of tolerances. As shown by the data, the internal system benefits greatly from kinematic mounts.

4. Conclusions

Comparison of the two fundus camera systems demonstrates the strengths and weakness of each design. The external system provides a unique approach to eliminating back reflections from the imaging optics. Only corneal back reflections are of concern for this particular configuration. The external design strategy allows for slightly better chromatic correction, eliminates the need for aspheric lenses in the imaging system, and allows for looser manufacturing tolerances. Despite these advantages, the illumination efficiency is severely reduced and is not suited for larger FOVs, due to the increase in lens' diameter. The internal design strategy offers a significant increase in illumination efficiency and a larger FOV for smaller lens' diameters. Neither shows a clear advantage in monochromatic image quality or accommodation of refractive error. When considering these designs for commercial production, the number and size of the optical elements are likely to be a significant factor. In this category, the internal system is able to produce better performance using fewer optical elements. Both design approaches demonstrate a great ability to image the retina effectively. Choosing between the two systems is ultimately a decision of what criteria is most important for the manufacturer and the consumer.

References

1. Shibata, N.; Torii, M. Fundus camera. U.S. patent. 6,654,553. Nov 25. 2003
2. Nanjo, T.; Kawamura, M. Fundus camera. U.S. patent. 5,742,374. Apr 21. 1998
3. Knoll, HA. Ophthalmic instruments. In: Kingslake, R., editor. *Applied Optics and Optical Engineering*, Optical Instruments Part 2. Vol. 5. Academic; 1969. p. 281-304.
4. Hammer M, Schweitzer D. Quantitative reflection spectroscopy at the human ocular fundus. *Phys. Med. Biol* 2002;47:179–191. [PubMed: 11837611]
5. Delori FC, Pflibsen KP. Spectral reflectance of the human ocular fundus. *Appl. Opt* 1989;28:1065–1077.
6. Atchison, DA.; Smith, G. *Optics of the Human Eye*. Butterworth-Heinemann; 2000.
7. Schwiegerling, J. *Field Guide to Visual and Ophthalmic Optics*. SPIE; 2004.
8. Thibos LN, Hong X, Bradley A, Cheng X. Statistical variation of aberration structure and image quality in a normal population of healthy eyes. *J. Opt. Soc. Am. A* 2002;19:2329–2348.
9. DeHoog, E.; Schwiegerling, J. Optimal parameters for retinal illumination and imaging in fundus cameras. Ophthalmic Optics Laboratory, University of Arizona, 1630 E. University Boulevard; Tucson, Arizona 85721, USA: are preparing a manuscript to be called
10. Liang J, Williams DR, Miller DT. Supernormal vision and high-resolution retinal imaging through adaptive optics. *J. Opt. Soc. Am. A* 1997;14:2884–2892.

11. Liang J, Williams DR. Aberrations and retinal image quality of the normal human eye. *J. Opt. Soc. Am. A* 1997;14:2873–2883.
12. Optimax Systems Inc.. Manufacturing tolerances.
<http://www.optimaxsi.com/0404/Products/Spheres.htm>
13. Kreicher Optics. Aspheric Design Guide for Manufacturability.
http://www.kreischer.com/aspheric_design_guide.htm
14. Kidger, M. *Fundamental Optical Design*. SPIE; 2001.
15. Escudero-Sanz I, Navarro R. Off-axis aberrations of a wide—angle schematic eye model. *J. Opt. Soc. Am. A* 1999;16:1881–1891.
16. Kidger, M. *Intermediate Optical Design*. SPIE; 2004.
17. Shannon, RR. *The Art and Science of Optical Design*. Cambridge; 1997.
18. CVI Melles Griot. Optical fabrication tolerances.
http://www.cvilaser.com/Common/PDFs/CVIMG-Capabilities_Matrix.pdf
19. Rochester Precision Optics. Traditional optics capability.
<http://www.rpoptics.com/TraditionalOpticsCapabilities.htm>

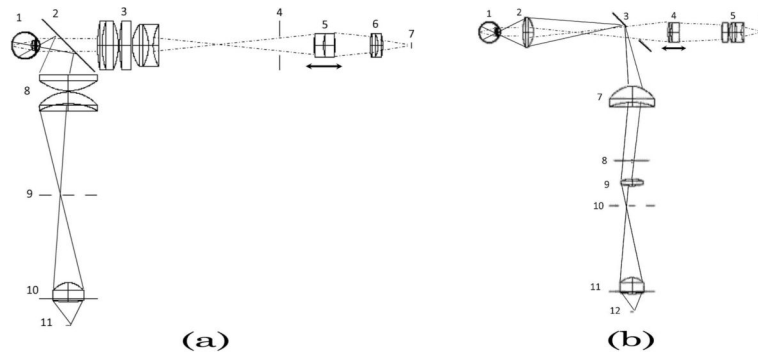


Fig. 1. Fundus camera system designed by the authors modeling schematics in the patent literature: (a) external illumination design and (b) internal illumination design.

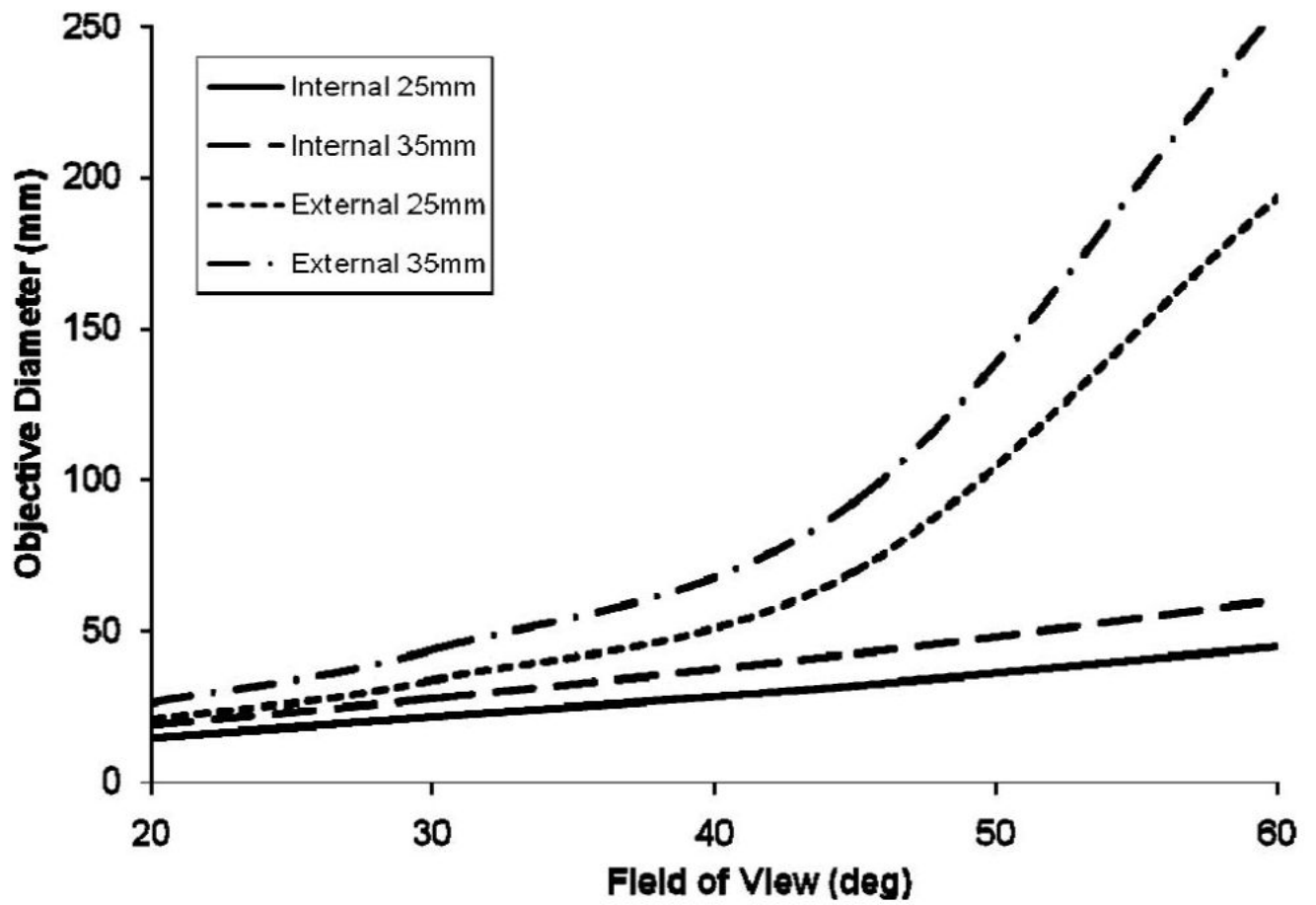


Fig. 2.
Objective diameter as a function of a FOV for working tances 25 and 35 mm.

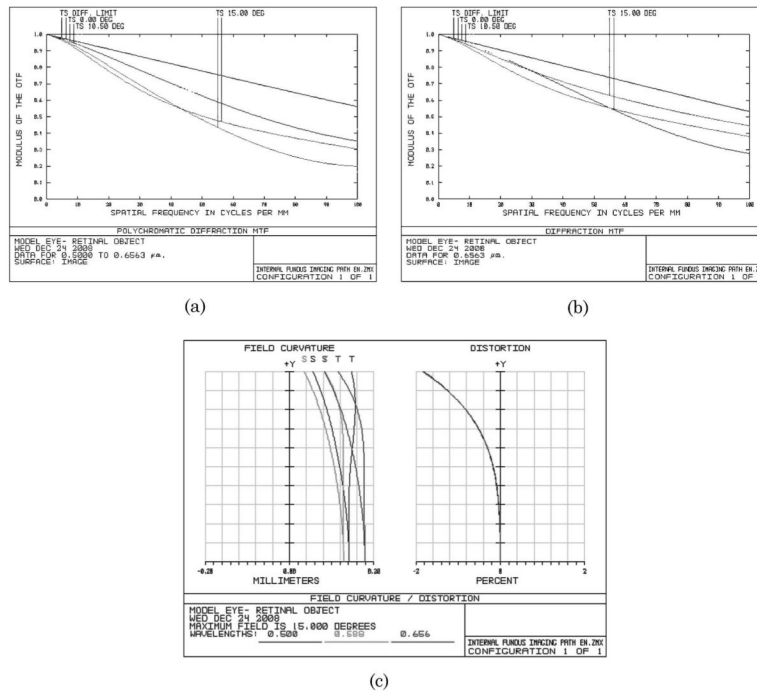
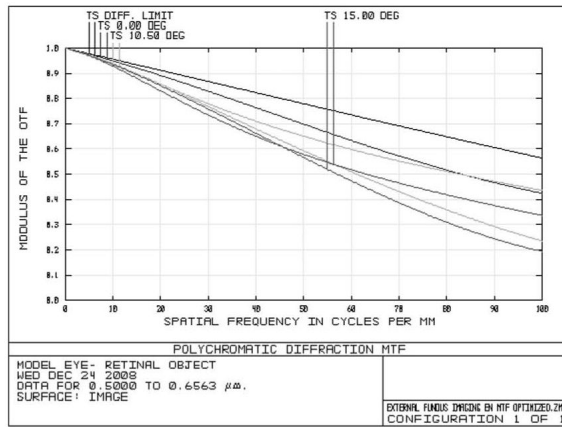
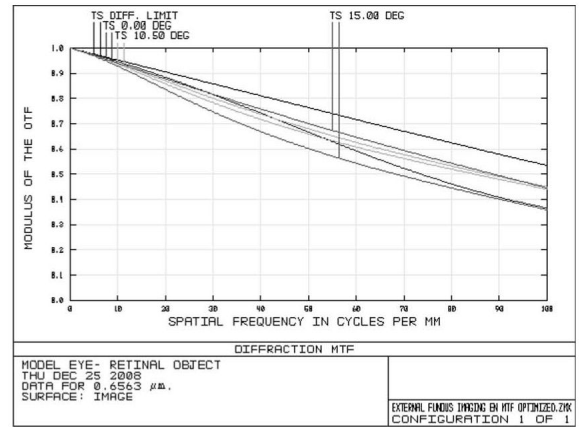


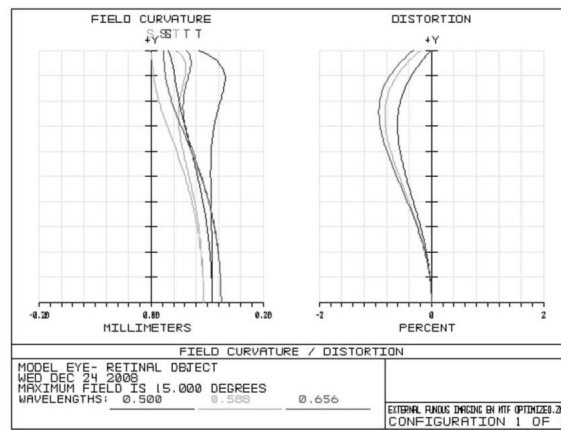
Fig. 3. MTF and field curvature of internal fundus camera system: (a) polychromatic MTF, (b) MTF at 656.3 nm, and (c) field curvature and distortion.



(a)



(b)



(c)

Fig. 4. MTF and field curvature of external fundus camera system: (a) polychromatic MTF, (b) MTF at 656.3 nm, and (c) field curvature and distortion.

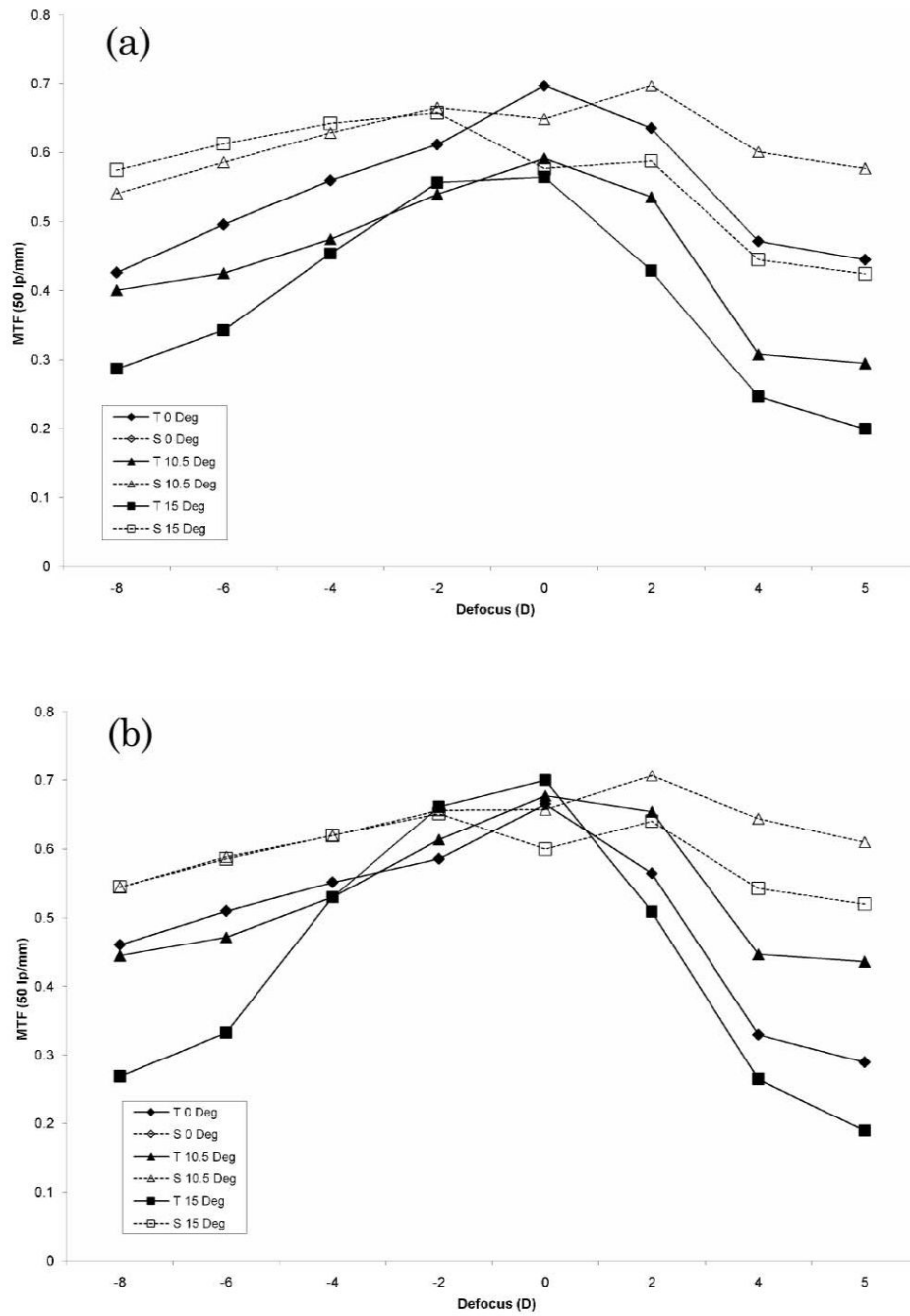


Fig. 5. External fundus camera defocus accommodations: (a) polychromatic MTF and (b) MTF at 656:3 nm.

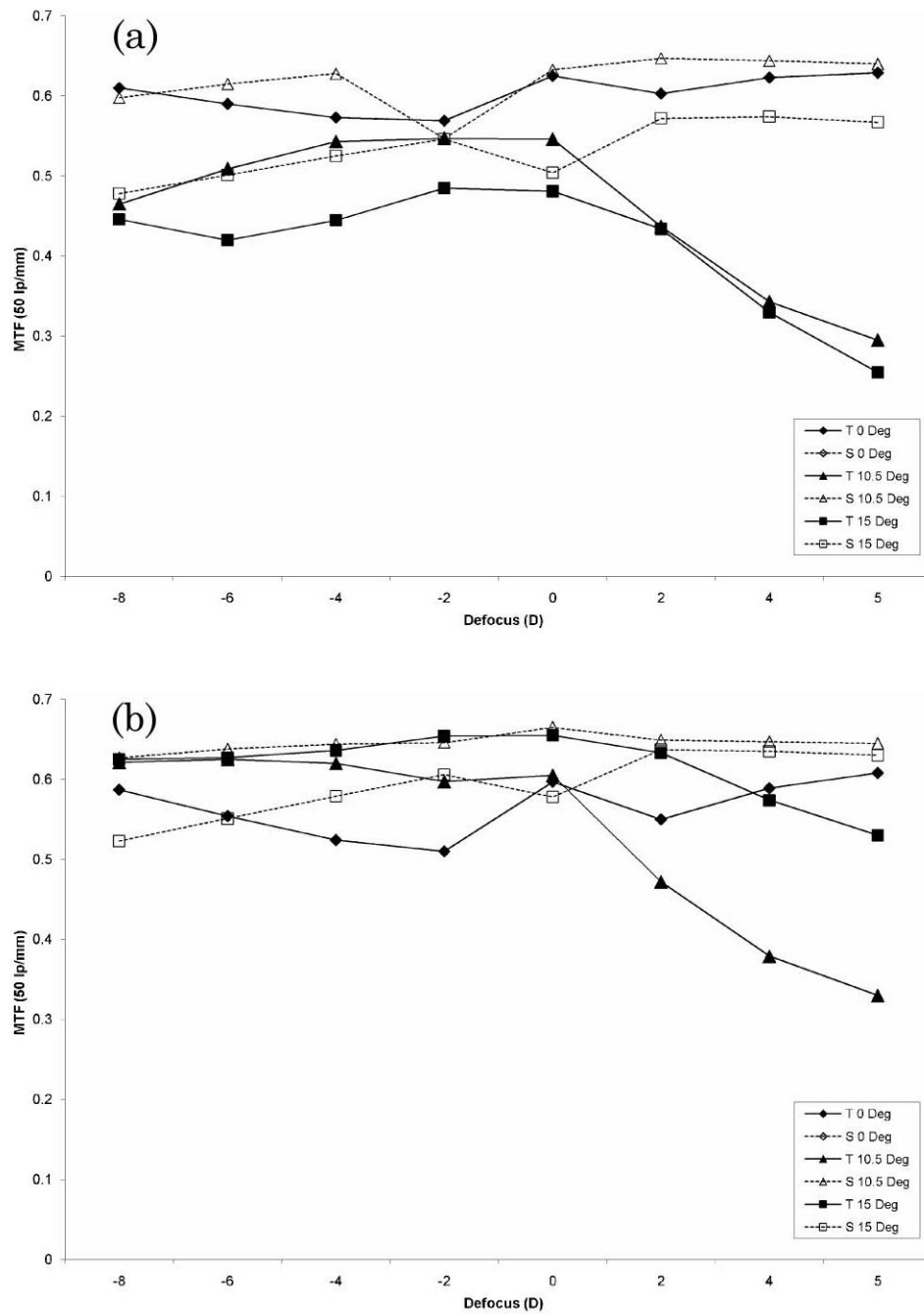


Fig. 6. Internal fundus camera defocus accommodation: (a) polychromatic MTF and (b) MTF at 656.3 nm.

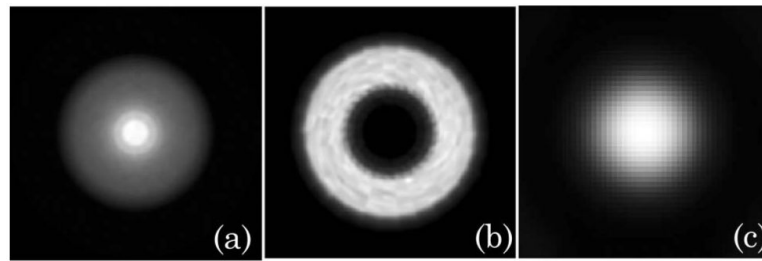


Fig. 7. Illumination patterns of the external system at (a) the retina, (b) the pupil of the eye, and (c) the CCD.

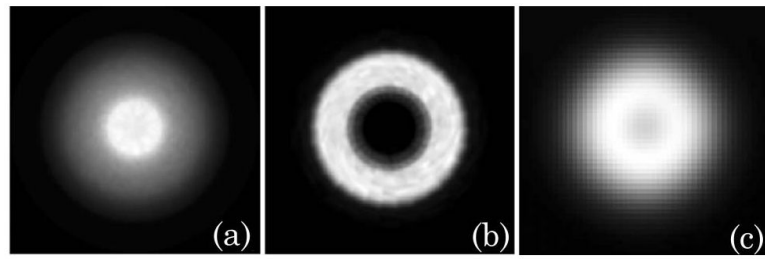


Fig. 8. Illumination patterns of the internal system at (a) the retina, (b) the pupil of the eye, and (c) the CCD.

Table 1
Travel of Zoom Lens Component for Accommodation of Defocus

Lens	External System		Internal System	
	5a	6a	4b	5b
-8D	-11.4 mm	-0.2 mm	-7.5 mm	-0.5 mm
+5D	13.5 mm	0.5 mm	5.9 mm	1.8 mm

Table 2
Efficiency Measurements for External and Internal Fundus Camera Systems

Source	External System		Internal System	
	Helical Filament	Lambertian Disc	Helical Filament	Lambertian Disc
η Source to Retina	19.2%	22.9%	39.3%	42.3%
η Retina to CCD	0.26%	0.43%	1.44%	1.85%
η Source to CCD	0.056%	0.106%	0.567%	0.784%

Table 3

Tolerance Values Selected for Fundus Camera Systems

Radius	Irrregularity	Sag	Thickness	Decenter	Surface Tilt	Abbe #	Index
2 Fringes	1 Fringe	10 μm	0.1 mm	0.1 mm	1 arcmin	1%	0.001

Table 4

Results of 100 Monte Carlo Trials of Fundus Camera Systems

Compensators	External System			Internal System		
	Defocus	Tip, Tilt, and Defocus	Defocus	Tip, Tilt, and Defocus	Tip, Tilt, and Defocus	
Nominal Criteria	0.5581	0.5581	0.4588	0.4588	0.4588	
Standard Deviation	0.021	0.011	0.0816	0.0816	0.0331	
90% >	0.4952	0.5221	0.3417	0.3417	0.4384	